Journal of Petroleum Science and Engineering 196 (2021) 107652

Contents lists available at ScienceDirect

Journal of Petroleum Science and Engineering

journal homepage: http://www.elsevier.com/locate/petrol

Temperature gradient and pH effects on S_{or} estimates from SWCT tests - The no buffer case☆

Tom Pedersen

Department of Tracer Technology, Institute for Energy Technology, P.O. Box 40, 2027, Kjeller, Norway

ARTICLE INFO

Keywords:
Sor
SWCT test
Ethyl acetate
Temperature gradient
pH
No buffer

ABSTRACT

Residual oil saturation (S_{or}) is the fraction of immobile oil that remains after a water flood. This information is important for calculating recoverable reserves and evaluating EOR campaigns. Single Well Chemical Tracer (SWCT) tests yield a near-well average S_{or} based on a large rock volume. Correctly performed and analyzed, SWCT tests yield reliable S_{or} estimates. There are, however, two important effects that commonly are ignored. One is cooling of the reservoir during injection of the cold brine resulting in decreased hydrolysis rate of the primary tracer. The other is the hydrolysis rate's pH dependence. To study these phenomena, we have developed a numerical model of an ethyl acetate SWCT test and applied it to a generic case with test and formation data based on published values. An analytical model is used to calculate how the brine injection temperature varies with time. The ethyl acetate hydrolyses into ethanol and acetic acid that lowers the pH and changes the hydrolysis rate. Any buffer capacity in the injected fluid or formation is neglected. Our model is the first ever to combine realistic temperature calculations with pH dependent ethyl acetate hydrolysis rate during a SWCT test. S_{or} is estimated from synthetic tracer production curves using the direct chromatographic separation equation as well as the mean residence time. A large number of simulations were performed to investigate how the S_{or} estimates vary with different model assumptions and input data. In all cases, both methods underestimate the true S_{or}, typically by 2–4% - in some cases significantly more. We demonstrate that neglecting dispersion in the wellbore during injection and production is warranted with the rock and test data used in this study.

1. Introduction

Residual oil saturation (S_{or}) refers to the immobile oil that remains after a water flood. It is defined as the fraction of pore space occupied by immobile oil. In water-wet rocks with a low viscosity oil, S_{or} may be reached after just one pore volume of water has been pumped through the reservoir, whereas in mixed-wettability rocks, thousands of pore volumes may be required before there is no more mobile oil left (e.g., Salathiel, 1973). A 98% or higher water-cut is considered a practical criterion for the oil to be virtually immobile (Deans and Majoros, 1980). Reliable estimates of S_{or} are important for calculating recoverable reserves, in decisions on whether Enhanced Oil Recovery (EOR) operations are suitable for further exploitation of a reservoir as well as in assessments of their effect (e.g., Al-Mutairi et al., 2015; Jin et al., 2015; Khaledialidusti and Kleppe, 2015; Al-Shalabi et al., 2017). Teklu et al. (2013) give a review of various methods to estimate S_{or}.

The Single Well Chemical Tracer (SWCT) method, pioneered in the late 60's by the Exxon Production Research Co. (Deans, 1971), yields an average S_{or} based on a large volume of rock, typically several hundred cubic meters, with a horizontal depth of penetration of ~3–12 m away from the well, and a vertical dimension of several meters. This large sampling volume, together with the ability to control the depth of investigation, may be considered the main advantages of the SWCT method relative to other techniques (coring, logging etc.) (Sheely and Baldwin, 1982). Deans and Majoros (1980) give an extensive overview of the SWCT method and Deans and Carlisle (2007) present an updated discussion of the method.

A SWCT test consists of four steps – injection, push, shut-in and production. The test starts with injection of a primary tracer like ethyl acetate dissolved in brine into the oil-bearing formation. The primary tracer has a finite distribution constant (partition coefficient) between the immobile oil and the brine. The tracer bank is then pushed further into the target formation by subsequent injection of tracer-free brine. Thereafter, there is a few (~1–12) days shut-in (pause) during which the primary tracer partially is converted into a secondary tracer by hydrolysis - ethanol in the case of ethyl acetate. The secondary tracer has a

☆ www.ife.no
E-mail address: tomp@ife.no.

https://doi.org/10.1016/j.petrol.2020.107652
Received 9 April 2020; Received in revised form 5 July 2020; Accepted 12 July 2020
Available online 22 July 2020

distribution constant close to zero, i.e., it moves with virtually the same velocity as the brine (a quasi-ideal water tracer). When production commences, both the primary and the secondary tracer move towards the well. The difference in distribution constants causes a chromatographic separation effect, so that the primary tracer is delayed relative to the secondary tracer. The concentrations of the two traces are monitored at the well and plotted as a function of produced volume or time. The lag between the two curves can then be used to estimate S_{or} (Deans, 1971; Tomich et al., 1973) – the larger the difference, the larger is S_{or}.

Properly conducted and analyzed, SWCT tests yield 'fair to excellent estimates of S_{or}' (Chang et al., 1988) in both sandstone and carbonate reservoirs with large variations in temperature, fluid salinity and rock properties. In favorable cases, an accuracy of about 2–3% is confirmed by laboratory results from pressure-core methods (Tomich et al., 1973). Many hundred SWCT tests have been performed worldwide.

Observed tracer concentrations in sandstones are often quite simple to interpret. Tests in carbonate formations typically exhibit a number of complications, including extreme dilution, long tracer curve tails and poor recovery (Deans and Carlisle, 1986). These may be caused by local heterogeneities (vugs, skeletal fragments) that prevent some of the pore space from being accessible to the flowing fluid. In such regions, transport of tracers is governed by diffusion. Several macroscopic models have been developed to account for this phenomenon, including 'dead-end' (e.g., Coats and Smith, 1964) and 'pore-diffusion' models (Deans and Carlisle, 1986). SWCT test simulations with more advanced models often yield a good fit to observed tracer curves also in carbonate reservoirs.

Storing and handling large volumes of flammable and volatile chemicals like ethyl acetate or other esters represent health and safety issues. Al-Abbad et al. (2016)discuss a new set of tracers with much lower detection limits than the conventional esters and the tracer volumes required in a SWCT test may hence be reduced by several orders of magnitude. The authors present a pilot SWCT project conducted in a carbonate reservoir where three of the new tracers were used in conjunction with ethyl acetate as primary tracers. Albeit the degree of hydrolysis of the new tracers was very low (only 1–5%) which is well below the lower limit of 10% recommended by Deans and Majoros (1980), Al-Abbad et al. (2016) arrived at S_{or} estimates close to the ethyl acetate estimate. The new tracers seem promising and their low volumes may offer interesting extensions of SWCT tests, but more tests must be conducted before any firm conclusions can be drawn on their real potential and benefits. Several alternative SWT methods have been suggested by various authors. Khaledialidusti et al. (2014) give an overview of such efforts. However, the classical ethyl acetate (and other esters like propyl formate) method is still dominant.

Notwithstanding, there are two potentially important processes that commonly are ignored in the planning and interpretation of a SWCT test - cooling of the reservoir during injection of relatively cold brine and the pH dependence of the primary tracer hydrolysis rate. This paper discusses these two mechanisms and their combined effects on S_{or} estimates.

Normally, the injected brine is colder than the oil bearing formation, and this causes reservoir cooling. Tezduyar et al. (1987), Park (1989), Park et al. (1990) and Park et al. (1991) developed non-isothermal convection-diffusion-reaction finite-element numerical models of SWCT tests solving for the primary and secondary tracer concentrations as well as temperature. They found that both the primary tracer and the thermal front are delayed relative to the water front. The primary tracer travels slowly because it spends some time in the immobile residual oil, and the thermal front because the brine is heated by the hotter rocks in the target formation. When the primary tracer bank and the temperature front travel with approximately the same speed, a temperature gradient develops across the primary tracer bank. Since the primary tracer hydrolysis rate increases exponentially with temperature, such a gradient will cause the peak of the secondary tracer to be located further away from the well than the peak of the primary tracer. Consequently, when production commences, the secondary tracer starts some distance behind the primary tracer. If this 'handicap' is not accounted for, the results will be that the time lag between the primary and secondary tracers, and thus S_{or}, is underestimated (e.g., Park, 1989).

In addition to ethanol, hydrolysis of ethyl acetate also produces acetic acid causing a reduction in pH. Wellington and Richardson (1994a) studied the effect pH may have on the hydrolysis of the primary tracer, and found that for SWCT tests in a carbonate-cemented California turbidite as well as in a Gulf Coast sandstone, most of the ethyl alcohol was produced during the injection and production phases, and not during shut-in, thus violating a basic tenant in the SWCT method (cf. Deans and Majoros, 1980). Taking pH dependent hydrolysis rate into account increased the S_{or} estimate in the carbonate-cemented California turbidite from about 20 to 40%, in agreement with an independent S_{or} estimate derived from a CO_2 SWCT test (Wellington and Richardson, 1994b). However, Deans and Ghosh (1994) modeled the same SWCT test and concluded that although pH effects did increase the volumes of ethanol during injection and production at the expense of that produced during shut-in, this did not much influence their S_{or} estimate (25% or less if taking account cross-flow and other complexities). We note that neither Wellington and Richardson (1994a) nor Deans and Ghosh (1994) took into account temperature effects caused by the SWCT tests. Regrettably, little work has subsequently been published on the effect of pH changes on S_{or} estimates. A notable exception is the work of Khaledialidusti and Kleppe (2018) who present 1D (single and two-phase) isothermal SWCT models that incorporate pH changes and their effect on hydrolysis rates and tracer concentrations. They take into account a number of geochemical reactions and examine both kinetic and equilibrium models. Khaledialidusti and Kleppe (2018) also present several forward models that illustrate how pH and concentration profiles across the radius of investigation depend on kinetics, calcite concentration, temperature (isothermal), soluble hydrocarbon-phase components like CO_2, shut-in time and initial ethyl acetate concentration. They conclude (their Fig. 10) that temperature is the parameter that affects pH variations most. Khaledialidusti and Kleppe (2018) in addition discuss two more specific cases – one is the California Turbidite case earlier presented by Deans and Ghosh (1994), the other is what they call a 'General Sandstone Reservoir' lean in calcite cement and an 'intermediate' brine buffer capacity. Unfortunately, they present tracer production curves only for the latter model (their Fig. 14) and they give no S_{or} estimate even in that case.

The objective of this study is to investigate the simultaneous effects of target formation cooling and the pH dependence of the primary tracer hydrolysis rate on S_{or} estimates from SWCT tests. To this end, we have developed a numerical model of a SWCT test and applied it to a generic case derived from published data. Since we in this approach know the true S_{or} value, it possible to investigate how various S_{or} estimates diverge from the correct value as a function of variations in model assumptions and input parameters. We also discuss temperature and dispersion effects in the wellbore used to inject the fluids into the target formation.

Any buffer capacity (i.e., the ability to resist pH changes) is neglected in this study. In many SWCT tests, the acetic acid will be buffered by buffering agents like bicarbonate in the injected fluid or by carbonate minerals like calcite in the reservoir rocks. If, however, the injected fluid is lean in buffering agents and the SWCT test is performed in a clean sandstone with no or very little calcite cement, there will be little or no significant buffering, and our results will be realistic, but probably not very common due to the abundance of calcite cement in sandstone reservoirs. Our 'no buffer' scenario is probably more common if such a fluid is used in a SWCT test performed in a carbonate reservoir. The reason is that most (80–90%) carbonate reservoirs are preferentially oil-wet (e.g., Høgnesen et al., 2005), and the weak acetic acid will then not get in contact with the (potential) carbonate buffer because this is shielded by the oil covering it (A. Krivokapic 2020; pers. comm.).

2. Model

Our starting point is the model presented in Park (1989). Since radial flow is typical for SWCT tests, it is numerically advantageous to have an axisymmetric model centered on the vertical wellbore (Fig. 1).

Such geometry makes it possible to take three-dimensional effects into account in a simple and efficient manner. Three horizontal rock units surround the well. The formation where we wish to estimate S_{or} is a permeable sandstone. Above and below this layer there are impermeable shales with equal thicknesses (model parameters are given in Table 1).

We assume, like Park (1989), Park et al. (1990) and Park et al. (1991) that the target formation and the adjacent impermeable layers are at thermal equilibrium ($T \equiv T_R$) when the calculations commence (Fig. 2).

This assumption will not be valid if the SWCT test *sensu stricto* follows pre-injection of a tracer free fluid. If that is the case, the thermal simulations have to start when the pre-flush begins. We note that pre-flushing may strip off light components in the residual oil, and thus change its composition as well as S_{or} (Gadgil, 1979; Deans and Majoros, 1980).

2.1. Fluid velocity

The injected brine flows into the permeable layer from the left (Fig. 2). For perfect radial flow of an incompressible fluid, the Darcy velocity $\vec{u}$, as a function of distance, r, from the center of the wellbore is (e.g., Park, 1989):

$$\vec{u} = \begin{pmatrix} u_r \\ u_z \end{pmatrix} = \begin{pmatrix} \frac{Q}{2\pi H r} \\ 0 \end{pmatrix} \tag{1}$$

in which Q is the pumping rate, H the thickness of the permeable layer

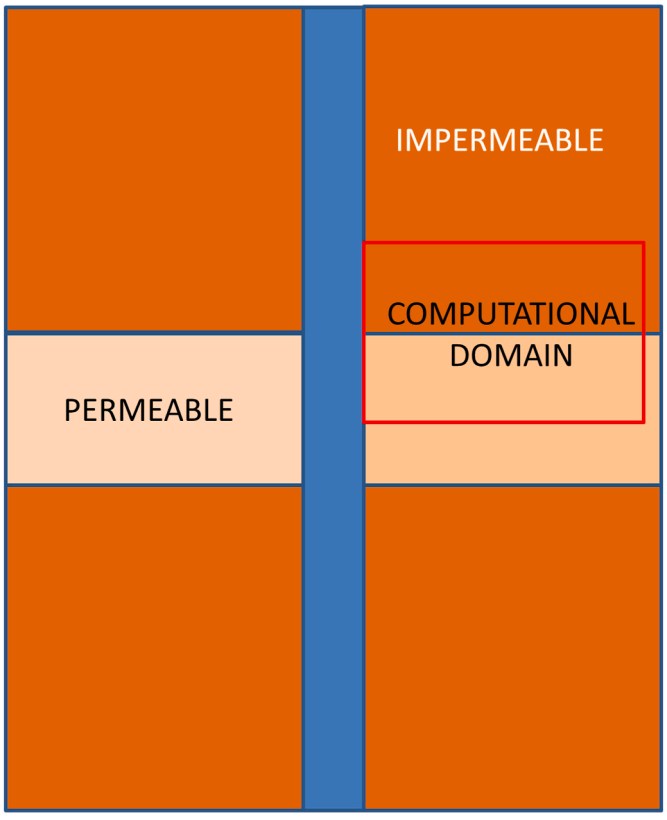

Fig. 1. The SWCT model configuration. The permeable target formation is surrounded by impermeable rock. Symmetry makes it possible to solve the equations only for the box labeled COMPUTATIONAL DOMAIN. The wellbore is in blue.

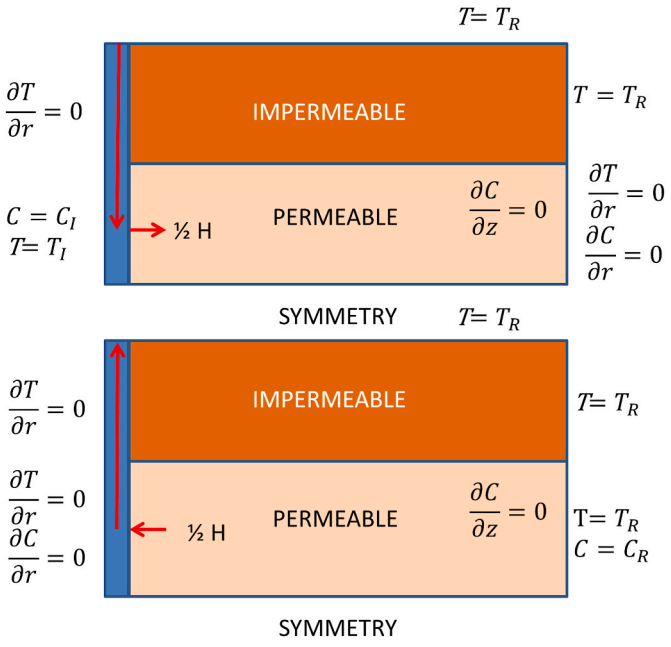

Fig. 2. Boundary conditions during injection (upper), shut-in and production (lower). Modified from Park (1989).

and r is distance from the wellbore center.

2.2. Temperature calculations

The temperature, T, during the SWCT test is governed by the heat equation:

$$(\rho C_p)_{eff} \frac{\partial T}{\partial t} + (\rho C_p)_w \vec{u} \nabla T = \nabla (k_{eff} \nabla T) \tag{2}$$

where the effective volumetric heat capacity (density, ρ, times specific heat, C_p)

$$(\rho C_p)_{eff} = \varphi \{ (\rho C_P)_{or,i} S_{or} + (\rho C_P)_w S_w \} + (1-\varphi)(\rho C_P)_r \tag{3}$$

where φ is porosity and the subscripts or,i, $_w$ and $_r$ refer to residual oil, water and rock, respectively and *i* is rock type – sandstone or shale.

$k_{eff,i}$ is the effective thermal conductivity equal to $(1-\varphi)k_{m,i} + \varphi k_w$, in which *i* represents the sandstone target formation or the shales above and beneath it, $k_{m,i}$ is the matrix thermal conductivity and k_w is the thermal conductivity of water. The difference in thermal conductivity between water and oil is for simplicity ignored (as did Park and co-workers). Taking oil explicitly into account would have reduced the total thermal conductivity with only about 1% in the sandstone formation with the parameters in Table 1 (in the shale formations, there is no oil). This has no significant bearing on our results. S is saturation. In a two-phase system, we have that

$$S_w = 1 - S_{or} \tag{4}$$

Parameter values are given in Table 1 and boundary conditions in Fig. 2. The injection temperature is illustrated in Fig. 3 (see Appendix A).

The perhaps most important feature in that figure is that, due to the assumption of steady-state conditions when the injection starts, there is a smooth decrease in the temperature of the injection fluid as it enters the target formation. If we had used an abrupt temperature increase like for example Park et al. (1991) did, our simulations show that it would have been difficult to avoid using unrealistically high dispersivity values to stabilize the combined temperature and pH dependent hydrolysis rate numerical calculations. More important is that such a smooth temperature change seems more realistic. Pedersen (2018) demonstrates how

Table 1
Symbols, values and descriptions.

Symbol	Value	Description
H	12 m	Target formation height
W	10 m	Model width
Z		Depth to formation
R		Radial distance
T		Time
t_i		Cf. Eq. 17
Qinj	450 bls/d	Injection rate
Qprod	480 bls/d	Production rate
C		Concentration
C_I	100 mol/m^3	Injection concentration (equilibrium)
C_R	0 mole m^{-3}	Reservoir concentration
D_F	10^{-9} m^2/s	Diffusivity
D_{Dr}		Radial dispersion
D_{Dz}		Vertical dispersion
T		Temperature
T_I	See Fig. 2	Injection temperature
T_R	73 °C	Reservoir temperature
Tinj	1 d	Injection period
Tpush	1 d	Push period
Tshutin	6 d	Shut in period
Tprod	6 d	Production period
Φ	23%	Target formation porosity
φ_{eff}		Effective porosity
T		Tortuosity
K	See text	Ethyl acetate hydrolysis rate (1/d)
k_a		Acid catalysis constant
k_b		Base catalysis constant
k*	10^(8.6–3469.1/T)1/d	Rate (1/d) (Deans and Majoros, 1980)
S_{or}	22%	Residual oil saturation
S_{or}*		Estimated Sor using Eq. 16
S_{or}**		Estimated Sor using Eq. 18
S_w		Water saturation
S_S	20 000 ppm	Salinity
U		Darcy velocity
V		Interstitial velocity
$(\rho C_p)_{eff}$		Effective volumetric heat capacity
$(\rho C_p)_{or}$	1.67 10^6 J/m^3/K	Oil volumetric heat capacity
$(\rho C_p)_{r,sandstone}$	2.20 10^6 J/m^3/K	Sandstone volumetric heat capacity
$(\rho C_p)_{r,shale}$	2.36 10^6 J/m^3/K	Shale volumetric heat capacity
$(\rho C_p)_w$	4.18 10^6 J/m^3/K	Water volumetric heat capacity
k_{eff}		Effective thermal conductivity
$k_{m,sandstone}$	3.0 W/m/K	Sandstone matrix thermal conductivity
$k_{m,shale}$	2.45 W/m/K	Shale matrix thermal conductivity
k_w	0.6 W/m/K	Water thermal conductivity
k_P		Adsorption isotherm
K		Distribution constant
A	0.021 K/m	Geothermal gradient
B	10 °C	Earth's surface temperature
T_0	10 °C	Water surface temperature
Cp,w	4180 J/K/kg	Injected fluid specific heat
r_0	0.1 m	Well radius
A	1.1 10^{-6} m^2/s	Thermal diffusivity of the Earth
α_r	10^{-3} m^2/s	Radial dispersivity
α_z	0.5 α $_r$	Vertical dispersivity
U		Fluid velocity in wellbore
v*		Friction velocity
K	10.1 r_0 U (v*/U)	Virtual diffusion coefficient

properly designed fluorescent nanoparticles co-injected with the primary tracer can yield information on the real temperature history during a SWCT test.

2.3. Chemical reactions and solute transport

Ethyl acetate ($C_4H_8O_2$) is the most common primary tracer used in SWCT tests. It hydrolyses to form the secondary tracer ethanol (C_2H_5OH) and acetic acid (CH_3COOH):

$$C_4H_8O_2 + H_2O \rightarrow C_2H_5OH + CH_3COOH \quad (5)$$

There are also two equilibrium reactions:

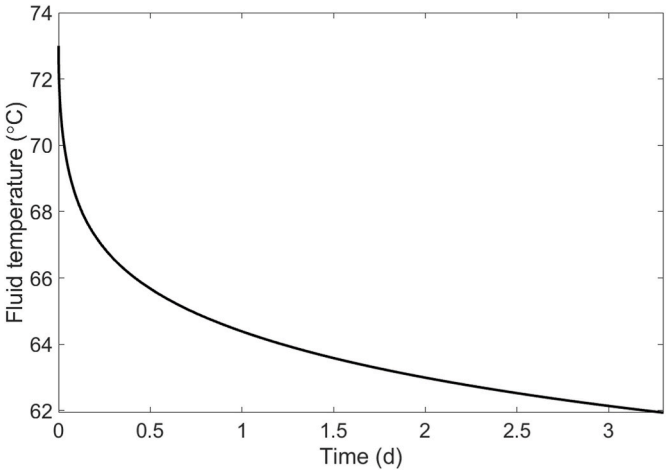

Fig. 3. Injection temperature as function of time derived from the equations in Appendix A with the parameters in Table 1.

$$CH_3COOH \leftrightarrow H^+ + CH_3COO^- \quad (6)$$

(in which CH_3COO^- is acetate) with the equilibrium constant K_{eq} (for concentrations in mole l^{-1} (i.e., M) – in the simulations we use the SI unit mole m^{-3}):

$$K_{eq} = 1.8 \cdot 10^{-5} \quad (7)$$

and

$$H_20 \leftrightarrow H^+ + OH^- \quad (8)$$

The water dissociation constant, K_W,

$$K_W = [H^+][OH^-] \quad (9)$$

depends on temperature (Fig. 4).

The ethyl acetate concentration in the brine is 100 mol m^{-3} (=0.1 M). Note that this is the ethyl acetate concentration when the ethyl acetate is at equilibrium between oil and brine. In the well, where there is no oil to partition to, the ethyl acetate concentration will be about 2.5 times higher with the parameters in Table 1. Since we are looking at the 'no-buffer' scenario, it is assumed that there is no calcium or carbonate species in the brine and the initial pH is therefore close to neutral (see also Ghosh (1994), his Simulation #4).

The transport of ethyl acetate and other solutes in the target formation follows the equation:

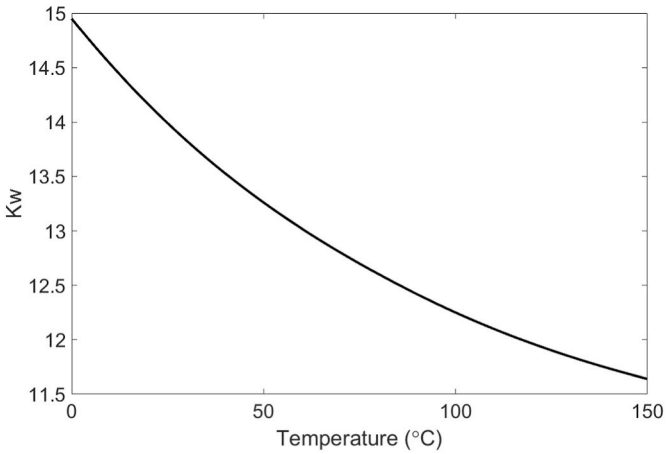

Fig. 4. Water dissociation constant Kw as a function of temperature. Based on Bandura and Lvov (2006).

$$(\varphi_{eff} + \rho_b k_{P,i}) \frac{\partial C_i}{\partial t} + \vec{u} \nabla C_i = \nabla \left[\left(D_{D,i} + \frac{\varphi_{eff}}{\tau_i} D_{F,i} \right) \nabla C_i \right] + \varphi_{eff} R_i \quad (10)$$

here, φ_{eff} is the effective porosity equal to $\varphi(1 - S_{or})$, ρ_b is the dry bulk density, $k_{P,i}$ is the adsorption isotherm, C is the concentration, $D_{D,i}$ is the dispersion, τ_i is the tortuosity, $D_{F,i}$ is the diffusivity, R_i is a reaction term and i refers to solute number i. For ethyl acetate $R = -kC_{ethyl\ acetate}$, whereas for ethanol and acetic acid, $R = kC_{Ethyl\ Acetate}$. The adsorption isotherm is

$$k_P = \frac{S_{or} \varphi K}{\rho_r (1 - \varphi)} \quad (11)$$

for ethyl acetate and zero for the other solutes. K is the distribution constant, ρ_r is rock density and the other terms have been defined earlier. We use the following expression for K (Deans and Majoros, 1980):

$$K = \left\{ 2.4 + \left(1.0 + \frac{S_s}{24,000} \right) (0.018T - 5.197) \right\} \quad (12)$$

where we have neglected K's dependency on the tracer concentration because this effect is small (Deans and Majoros, 1980). S_s is salinity measured in ppm while temperature is measured in Kelvin. The boundary conditions for the solute transport calculations are given in Fig. 2. We assume that the initial concentration (neutral pH) of H^+ and OH^- in the target formation follows the curve in Fig. 3.

The overall reaction rate for the hydrolysis of ethyl acetate to ethanol, k, depends on $[H^+]$ and $[OH^-]$ (International Critical Tables, first edition, 1930):

$$k = k_a[H^+] + k_b[OH^-] \quad (13)$$

in which k_a and k_b are the acid and base catalysis constants, respectively. Fig. 5 illustrates k as a function of pH and temperature.

We calculate the tortuosity from the Millington and Quirk (1961) formula $\tau = \varphi^{-1/3}$. For the porosity in Table 1, this yields 1.6. Dispersion is calculated from the expressions (Bear, 1979):

$$D_{Dr} = \alpha_r \frac{u_r^2}{|u|} \quad (14)$$

and

$$D_{Dz} = (\alpha_r - \alpha_z) \frac{u_z^2}{|u|} \quad (15)$$

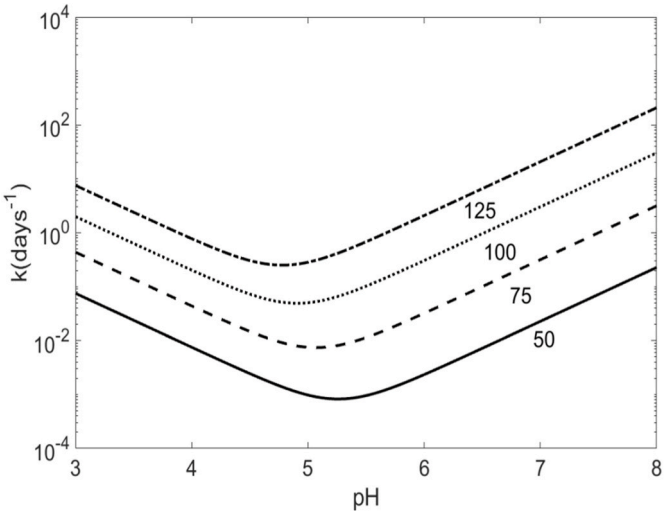

Fig. 5. Hydrolysis rate of ethyl acetate as function of pH and temperature in °C. Based on International Critical Tables (1930).

where α_r and α_z are the radial and vertical dispersivities, respectively.

The set of equations above are solved using the commercial finite element PDE software COMSOL Multiphysics (2018). The mesh consists of triangular elements with higher resolution near the well since that is where most of the variations take place. Time stepping is performed by a second order implicit backward differentiation formula (BDF). It takes typically between five and 10 min to solve a model on a 64 bit computer with two processors and 128 GB RAM memory.

The most important difference between our model and the models published by Khaledialidusti and Kleppe (2018) is probably that we have a realistic 3D description of the temperature changes during a SWCT test whereas their models are isothermal. That the assumption of constant temperature during a SWCT test is almost universally used in the literature on SWCT tests does not make it any more realistic. Because temperature governs the hydrolysis rate of ethyl acetate and other esters, induced pH changes and distribution constants, a sound model of temperature changes during a SWCT test is of the utmost importance. The important 'handicap' (horizontal separation between the ethyl acetate and ethanol tracer curves when production commences) identified already by Park and co-workers around 1990 cannot be studied in isothermal models. Furthermore, our model has a radial velocity field representative for (most) SWCT tests while Khaledialidusti and Kleppe (2018) use a 1D transport equation. We take into account diffusivity and dispersion. These effects are ignored by Khaledialidusti and Kleppe (2018).

2.4. Test and formation data

We define a generic or representative SWCT test and rock data set (Table 1) based on Park (1989) as well as Table 5-1 in Deans and Majoros (1980). Their table contains data from 59 SWCT tests mostly in sandstones although a few limestone cases are included as well. Since we use ethyl acetate as primary tracer in our calculations, the initial reservoir temperature was based on the ethyl acetate SWCT tests only, i.e., we exclude those SWCT tests in which the reservoir temperature is too low for sufficient hydrolysis of ethyl acetate during the test.

2.5. Sor estimates

S_{or} is estimated from the synthetic tracer concentration curves using two methods. The first is the direct application of Cook (1971) chromatography formula:

$$S_{or}^* = \frac{t_{Etyl\ Acetate} - t_{Ethanol}}{t_{Etyl\ Acetate} + t_{Ethanol}(K - 1)} \quad (16)$$

in which t is the time when the concentrations of ethyl acetate or ethanol are at their maximum and K is again the distribution constant.

One of the assumptions in Eq. (16) is that dispersion of the tracers is negligible. In a real SWCT test, there will be dispersion. Deans and Majoros (1980) suggested to use the ratio between the first and zero statistical moments (i.e., the mean residence time) defined as

$$\overline{t_i} = \frac{\int_0^\infty t\ C_i dt}{\int_o^\infty C_i dt} \quad (17)$$

to account for dispersion in SWCT tests; i stands for ethyl acetate or ethanol. The estimated value of S_{or} obtained by inserting the times from Eq. (17) into Eq. (16), i.e.,

$$S_{or}^{**} = \frac{\overline{t_{Etyl\ Acetate}} - \overline{t_{Ethanol}}}{\overline{t_{Etyl\ Acetate}} + \overline{t_{Ethanol}}(K - 1)} \quad (18)$$

is referred to as the Residence Time Distribution (RTD) estimate. Dispersion will broaden the ethyl acetate as well as ethanol tracer concentration curves as they move towards the producer and the peaks in the curves will no longer be representative for the average times the

tracers have spent from the production commences until they reach the producer. Eq. (18) may yield as better S_{or} estimate in such a situation provided a number of assumptions are fulfilled including no chemical reactions (e.g., Asakawa, 2005). Shook et al. (2009) demonstrate the potential of using residence time distributions and not only the residence time mean in estimates of flow geometries, swept volumes and residual (as well as remaining) oil saturation in inter well tracer tests in synthetic reservoirs with variable porosity and permeability. Their models, however, do not include temperature or pH changes and their effects on the S_{or} estimates. As we now will show, in SWCT tests with realistic temperature histories, pH changes and variable distributions constants in addition to tracer dispersion, S_{or}* sometimes yields better estimates than S_{or}** and sometimes the opposite is true.[2–6] In both Eqs. (16) and (18), we use the distribution constant for the reservoir temperature T_R. This is a common assumption and is actually the only temperature value available without performing temperature calculations (see also Discussion).

3. Results

Fig. 6 illustrates simulation results using the test and formation data in Table 1.

Fig. 6A demonstrates that the ethyl acetate moves with a velocity of about 1.5 m per day. Assuming that the sandstone grains have a diameter of 200 μm and that ethyl acetate has a chemical diffusion constant equal to 10^{-9} m^2s^{-1}, we arrive at an average Peclet number of about 4. Close to the well, the Peclet number will be higher and more distantly lower. From Fig. 7.4 in Bear (1979), we adopt a value of 10^{-3} for α_r and 0.5 α_r for α_z in Eq. (14) and15, respectively. We see that there is a temperature gradient across the ethyl acetate primary tracer bank and that the ethanol secondary tracer is displaced away from the wellbore, i.e., the 'handicap' discussed by for example Park (1989). This will reduce S_{or} if estimated by either Eq. (16) or 18 since they are based on the assumption that there is no lateral displacement between the primary and secondary tracer when production starts (e.g., Deans and Majoros, 1980). Fig. 6B depicts pH. Its minimum value is close to the theoretical minimum (~2.7) when all the ethyl acetate has been converted to ethanol and acetic acid. It follows from Fig. 5 that the ethyl acetate hydrolysis rate is slightly higher than for the initial pH of about 6.5. The large reduction in hydrolysis rate for pH around 5–6 during shut-in, and the consequences thereof, as discussed by Wellington and Richardson (1994a) is thus not observed in our simulation results. The reason is that we assume that there is no buffer capacity neither the in injected fluid nor in the oil bearing formation. These results agree with those reported by Ghosh (1994; his simulation #4). The pH curve in Fig. 6B is also consistent with pH results presented in Khaledialidusti and Kleppe (2018) (their Fig. 12B), although their minimum pH is about 3.4 while ours is slightly less than 3. This is as expected as they model 'a general sandstone' with some brine buffer capacity whereas we model a 'no buffer' case. In Fig. 6C, we note that the ethyl acetate hydrolysis rate varies by one order of magnitude across the primary tracer bank and that its maximum is approximately 15 times higher than the much used rate

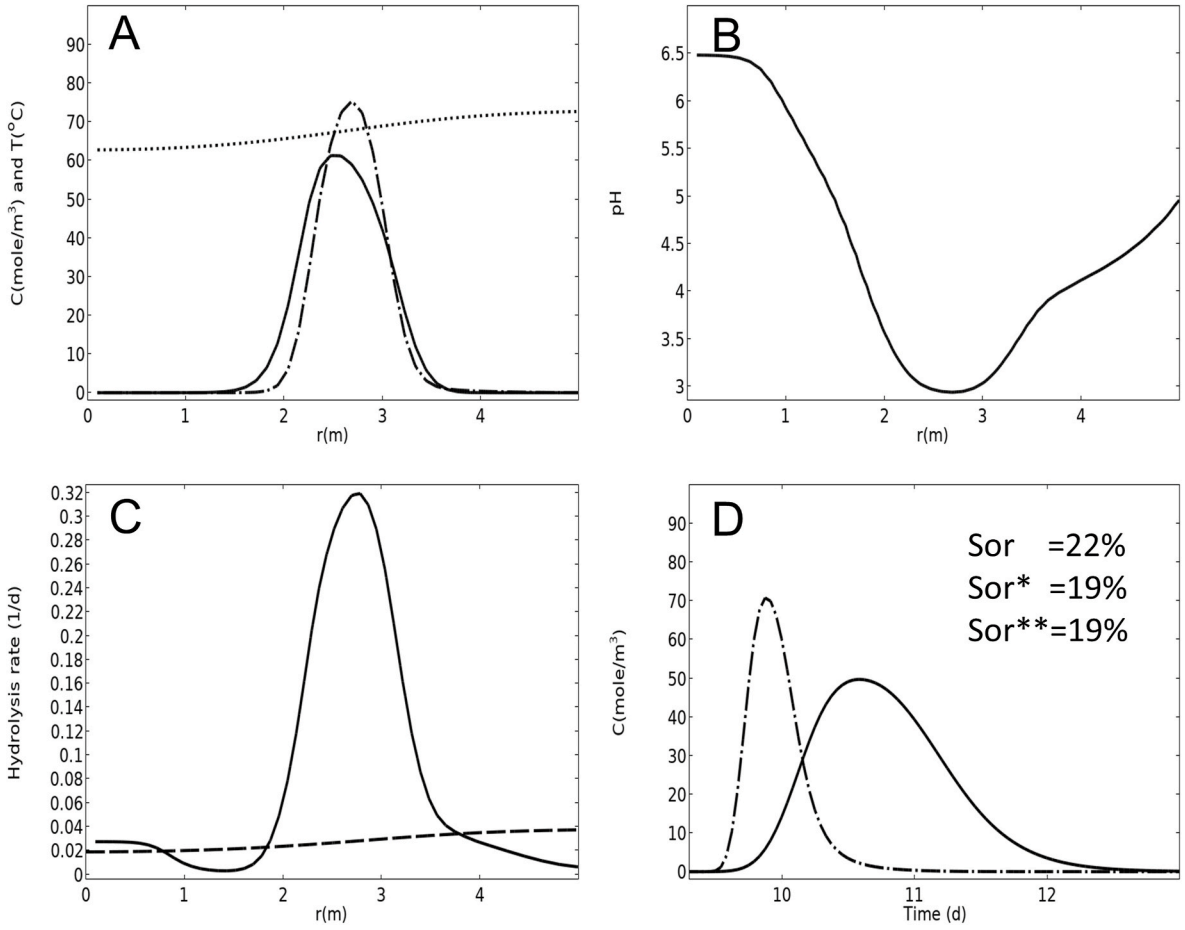

Fig. 6. A–C: Results at the end of the shut-in phase (9.3 days) as functions of distance from the center of the wellbore. (A). Solid line: ethyl acetate concentration. Dashed line: ethanol concentration. Dotted line: temperature. (B) pH. (C) Solid line: hydrolysis reaction rate k. Dashed line: the widely used hydrolysis reaction rate k* (e.g., Deans and Majoros (1980). (D) Tracer production curves starting at 9.3 days. Sor is the true residual oil saturation whereas Sor* and Sor** are the estimated values using Eq. (16) and Eq. (18), respectively. Since both the ethyl acetate and ethanol curves are quite symmetrical, applying Eq. (18) instead of Eq. (16) has no appreciable effect.

presented by Deans and Majoros (1980). Since the formation and test data used in the calculations are averages from a rather large number of various SWCT tests, we would argue that the common assumption of a constant hydrolysis rate used in most SWCT test models (e.g., Deans and Majoros, 1980; Jerauld et al., 2010; Jin et al., 2015) is an over-simplification. It is, however, beyond the scope of this study to evaluate the S_{or} estimate errors this might cause. Finally, Fig. 6D shows synthetic tracer curves, i.e., the primary and secondary concentrations at the production outlet (Fig. 2). Applying Eq. (16), probably the most widely used method to estimate S_{or}, we find that S^*_{or} is about 19%, i.e., three percent lower than the true S_{or} value of 22% (Table 1). RTD (Eq. (18)) yields the same estimate. We repeated the calculations with ethyl acetate (equilibrium) injection concentrations equal to 40 and 20 mol m^{-3}. Although the tracer curves do differ (not shown), the S_{or} estimates changed by no more than 1%. This indicates that perhaps the use of more realistic SWCT simulators could reduce the volume of primary tracers required for a successful test and thus minimize its environmental impact as well as any changes in S_{or} caused by the SWCT test itself (e.g., Gadgil, 1979).

It is essential to investigate the sensitivity of S_{or} estimates to variations in test and formation data. Fig. 7A and B illustrates how the estimated value varies as a function of reservoir temperature.

We see that the error (i.e., the difference between the estimated value and the true value of 22%) decreases with higher reservoir temperature. In Fig. 7B we note that the ethanol concentration is higher than the initial ethyl acetate concentration of 100 mol m^{-3}. This is because 'new' ethyl acetate is released from the oil into the brine during hydrolysis in order to keep K constant (Eq. (12)). In Fig. 7C, we see that the error in the estimated S_{or} value increases when the injection rate is doubled whereas Fig. 7D shows that the error is reduced when the injection rate is reduced by 50%. We note from Fig. 7 (as well as from Figs. 8 and 9 below) that in some cases Eq. (16) yields the best estimate of S_{or}, whereas in other cases Eq. (18) gives the best result.

Fig. 8 depicts the variations in estimated S_{or} values as a response to variations in shut-in time as well as in the true S_{or} value itself.

When the shut-in is reduced to three days (Fig. 8A), Eq. (16) underestimates S_{or} by 5% whereas Eq. (18) underestimates S_{or} by 6%.

Fig. 8B illustrates that when the shut-in is increased to 9 days. Eq. (16) yields a 4% too low estimate of S_{or} whereas Eq. (18) yields a 3% too low estimate. When the true S_{or} value is 11% (Fig. 8C), Eq. (16) yields an S_{or} estimate of only 6%. Such a large discrepancy may mislead oil companies to make the wrong economic decisions. However, estimating S_{or} with Eq. (18) gives 9%, i.e., an error equal to 'only' 2%. In the case that the true S_{or} is 33%, we note that Eq. (18) results in a slightly larger error than Eq. (16).

The results presented so far are for the 'full' mode, i.e., the model that takes into account both temperature variations and pH effects caused by the production of acetic acid during hydrolysis of ethyl acetate. Fig. 9A again illustrates synthetic production curves for the standard case (identical to Fig. 6D.)

Fig. 9B, however, shows the production curves for a model in which only the hydrolysis rate changes caused by pH variations are considered. Since in this scenario one of the complications (the temperature effects) is ignored, the estimated S_{or} values of 21 and 20% are closer to the true

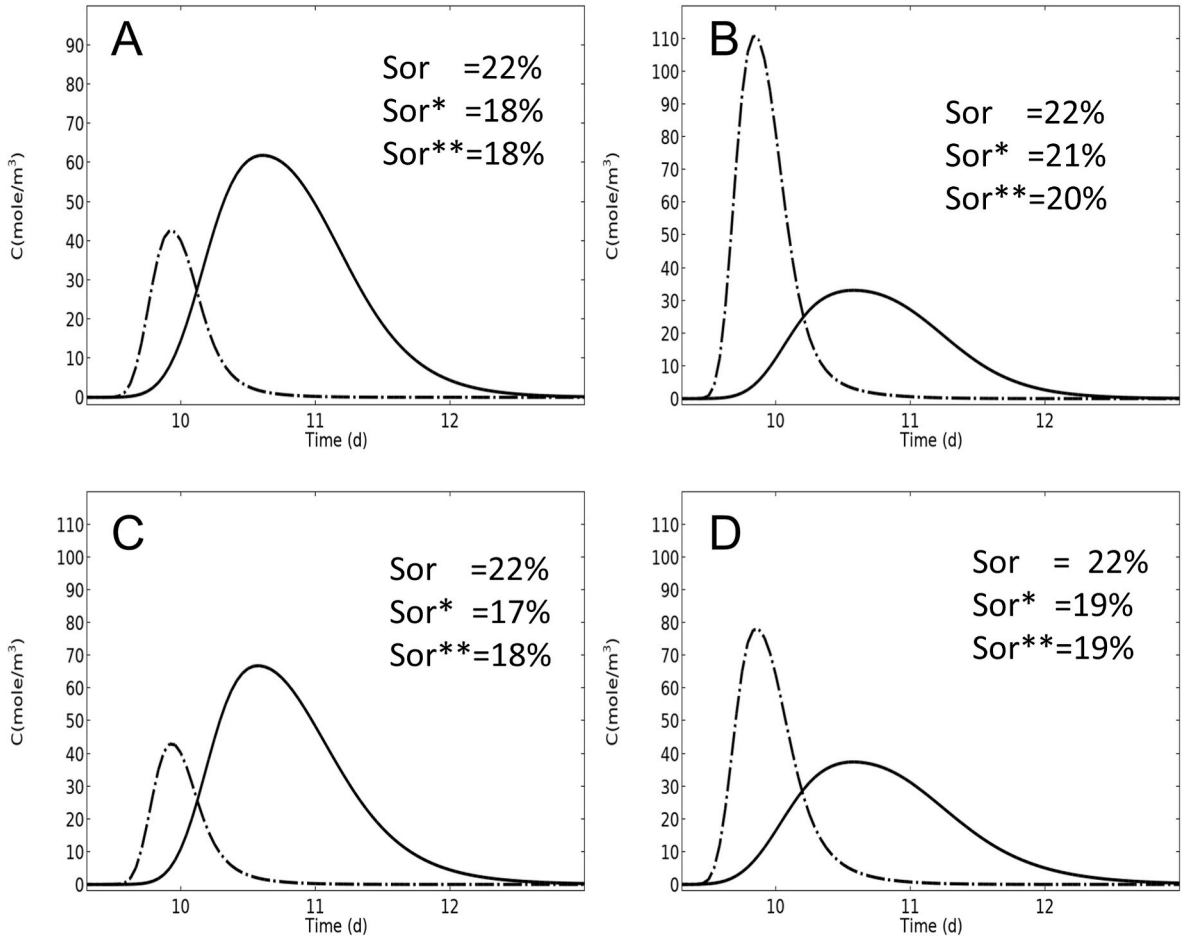

Fig. 7. Sensitivity of the tracer production curves to reservoir temperature and injection/concentration rates. Ethyl acetate: solid line - ethanol: dashed line. (A) Reservoir temperature is 63 °C. (B) Reservoir temperature is 83°. (C) Injection and production rates are twice as high as in Table 1 (D) Injection and production rates are 50% of those in Table 1.

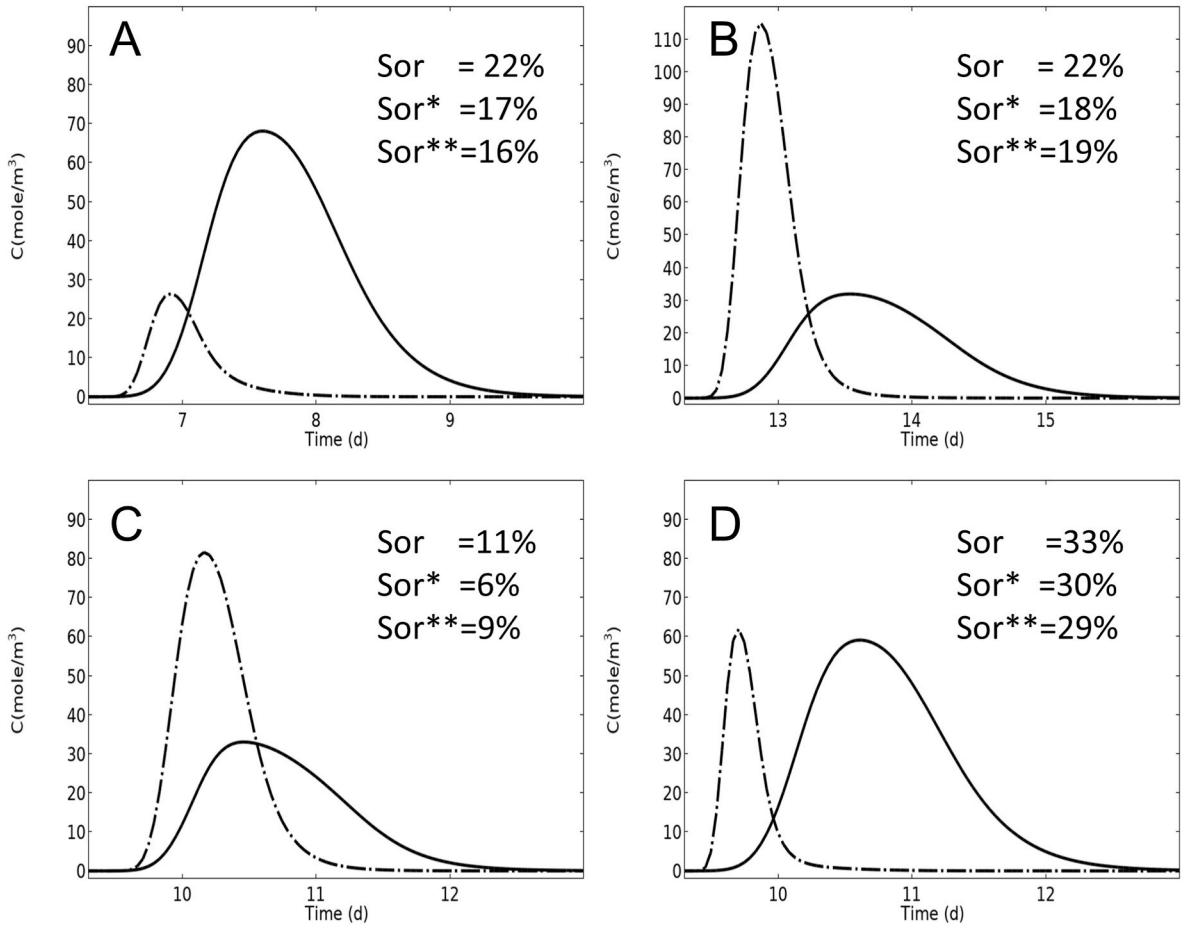

Fig. 8. Sensitivity of the tracer production curves to duration of shut-in and true S_{or}. Ethyl acetate: solid line - ethanol: dashed line. (A) Shut-in lasts 3 days. (B) Shut-in lasts 9 days. (C) Sor = 11%. (D) Sor = 33%.

value of 22%. There are two potential reasons why there still is a small error. Firstly, although there is no temperature gradient across the tracer bank, there is nevertheless a small 'handicap' between the primary and secondary tracer concentrations when production commences (not shown). This is because some hydrolysis does take place during the injection phase and the produced ethanol moves faster away from the wellbore than the primary (partitioning) tracer does. Secondly, Eq. (18) may not compensate 100% for the dispersion effect. We made no efforts to evaluate the relative importance of these two explanations since anyway the error must be considered small. The synthetic production curves when the temperature variations are included but not the pH effects on the hydrolysis rate are illustrated in Fig. 9C. The estimated value of S_{or} using Eq. (16) is (20%) is close to the true value (22%); however, Eq. (18) is this case seriously underestimates S_{or} yielding a value of only 13%, i.e., 9% below the true value. Finally, we see in Fig. 9D the production curves from a model where neither temperature nor pH effects are accounted for. The S_{or} estimate obtained with Eq. (16) (21%) is excellent whereas Eq. (18) gives only 15%. We note that the fractions of ethanol generated in Fig. 9C and D are small. Moreover, the ethanol curves are more skewed (more distorted to the right) than the ethyl acetate curves. Applying Eq. (18) will thus decrease the corrected differences between the two curves and this will reduce the estimated S_{or} value.

We note from Figs. 7–9 that Eqs. (16) and (18) always underestimate the true value of 22% S_{or}. Eq. (18) is thus unable to compensate for the 'handicap' (i.e., the horizontal separation between the ethyl acetate and ethanol tracer curves when production commences) (cf. Fig. 6A) in the scenarios that we have investigated. More work is needed to better understand why in some cases Eq. (16) yields the best result and in others Eq. (18) does so.

4. Discussion

In this paper, we have injected brine with the primary tracer directly into the formation rock (Fig. 2) and also calculated the production curves at the same location. This appears to be an almost universally accepted simplification. However, in a real SWCT test, injection is performed via a wellbore from the surface down to the oil bearing target formation. During production the flow takes place in the opposite direction. The question is then what consequences this simplification has. To study this problem, we have numerically solved the one dimensional diffusion and transport equation with the diffusivity defined by a formula derived by Taylor (1954) (cf., Appendix B) for turbulent flow (The Reynolds number is about 5600 with the parameters in Table 1). Fig. 10A illustrates the ethyl acetate concentration curves at the surface and at 3000 m depth where the target formation is located.

We note that there is only an insignificant difference (in shape – for simplicity we haven't taken the concentration difference caused by partitioning into account because this simply amounts to multiplying the values with about 2.5). Consequently, starting the injection calculations at the wellbore/target formation interface does seem warranted in our case. There may, of course, be other SWCT tests where this is not true. Fig. 10B and C depict the ethyl acetate and ethanol concentrations at the interface (Fig. 2) as well as at the top of the wellbore. Again, there is only an insignificant difference between the curves. Calculating S_{or} at the interface between the wellbore and the oil bearing formation (Fig. 2), or at the top of the wellbore as in a real SWCT test yields virtually the same value.

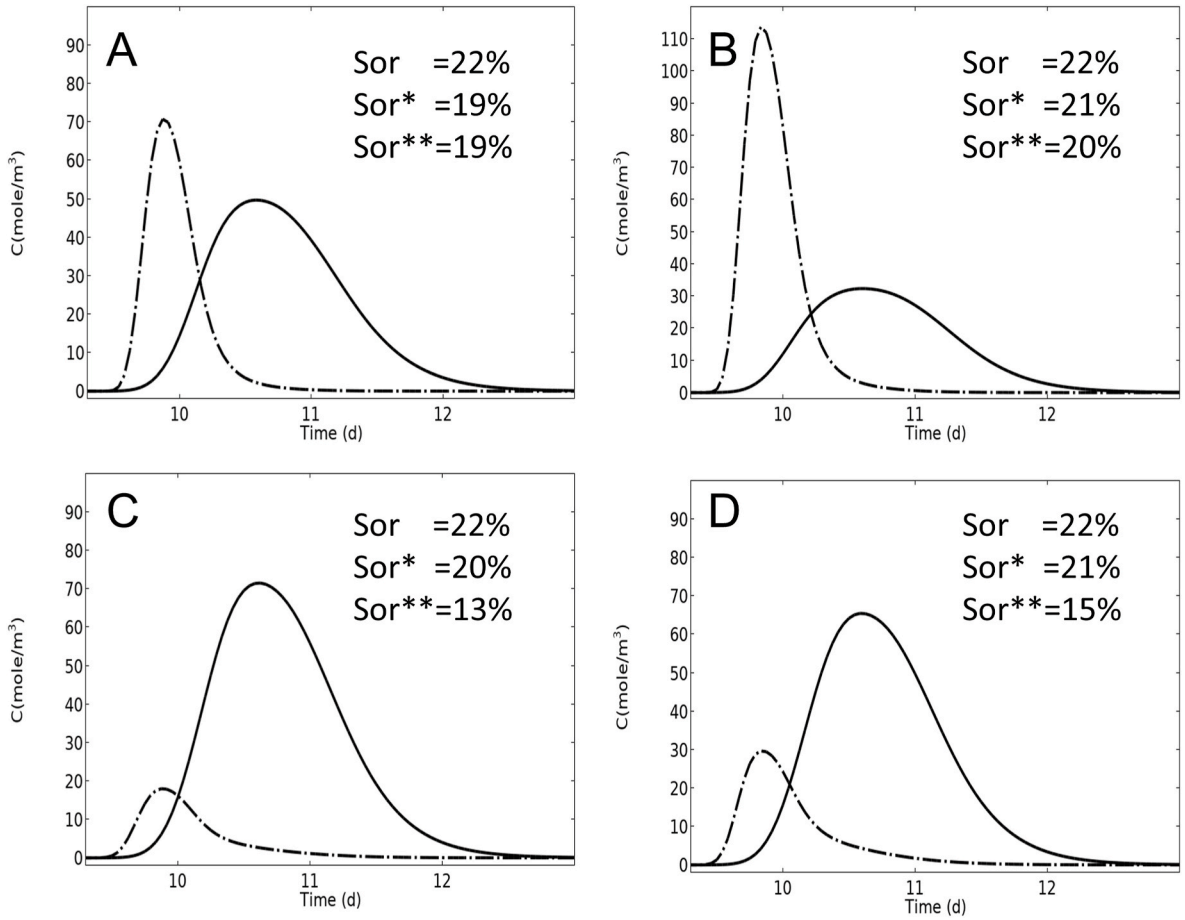

Fig. 9. Tracer concentration curves during the production phase for various model types. Ethyl acetate: solid line - ethanol: dashed line.(A) Full model, i.e., temperature as well as pH varies. (B) Isothermal model, i.e., only pH varies. (C) Temperature varies and pH is constant except for the variation in Kw (Fig. 4). (D) Neither pH nor temperature varies.

We do not observe the same detrimental consequences neglecting pH dependent hydrolysis rate has on S_{or} estimates as Wellington and Richardson (1994a) did in their study. This is probably due to the much larger pH decrease due to formation of acetic acid we find than Wellington and Richardson (1994a) did (pH falls to 6–6.5 during shut-in). For pH in the 6–6.5 range, the acetate ester hydrolysis rate is close to its minimum (Fig. 5). The volume of ethanol generated during shut-in is thus reduced relative to the volume produced during transit (injection, push and production). When transit (injection, pause and production) generated ethanol dominates over ethanol produced during shut-in, a SWCT test becomes insensitive to S_{or} (Deans and Majoros, 1980; Wellington and Richardson (1994a)). Because pH is our study gets much lower during shut-in, the hydrolysis rate is much higher (Fig. 5) and the sensitivity is better.

Unfortunately, it is not common to measure, or at least to publish, pH measurements from SWCT tests. There are, however, some papers where pH variations during the production phase are reported. Causin et al. (1990) present pH data from the well head in two SWCT tests. In the Chuelles field in France, pH was found to vary between 6.8 and 7.4, whereas the test in the Cortemaggiore field in Italy showed pH variations between 4.3 and 5.3. It is important to note that because of possible corrosion reactions in the wellbore (Wellington and Richardson, 1994a), pH might have been lower where the fluid leaves the target formation, i.e., where we present our calculated pH values. In a carbonate-cemented California turbidite SWCT test, Wellington and Richardson (1994a) observed a very high pH around 11 in the first returns – thereafter the pH dropped to between 6 and 7. It would be useful if more pH measurements were published from SWCT tests. Such measurements could provide an additional constraint on S_{or} at a moderate cost.

The efficiency of an EOR campaign may be assessed by comparing the S_{or} estimates before and after using two SWCT tests (e.g. Jin et al., 2015). Since the first SWCT test as well as the EOR operations themselves will disturb the temperature as well as chemistry in the target formation, it may be that the errors caused by ignoring temperature gradient and pH effects are different for the pre- and post EOR SWCT tests. The efficiency of an EOR operation might therefore to some extent be an artifact. We note that the first SWCT test may itself reduce S_{or} (e.g. Gadgil, 1979), and if this factor is not taken into account, one may misinterpret the effectiveness of an EOR campaign.

Khalediallidusti and Kleppe (2017) propose a design methodology for SWCT tests that combine analytical and numerical methods in the quest for designs that minimize deviations from an 'ideal' test case, thus reducing the need for taking into account pH changes etc. We agree with Khalediallidusti and Kleppe (2017) in that such designs may provide interesting and useful insights into SWCT tests, their planning and analysis. However, it seems much simpler, more straightforward and economical to combine a model like the one presented in this paper with inversion methods (see also Huseby et al. (2016)) to obtain reliable S_{or} estimates. In particular, it is very difficult to understand how an isothermal SWCT test can possibly be realized. This would seem to require almost infinitely low injection and production rates in order not to disturb the temperature in the rocks surrounding the wellbore. The cost of such a hypothetical test would be astronomical and no useful results would probably be obtained since all the ethyl acetate would have been hydrolyzed and diffusion would have spread the ethanol evenly. Perhaps combining a design approach ala Khalediallidusti and

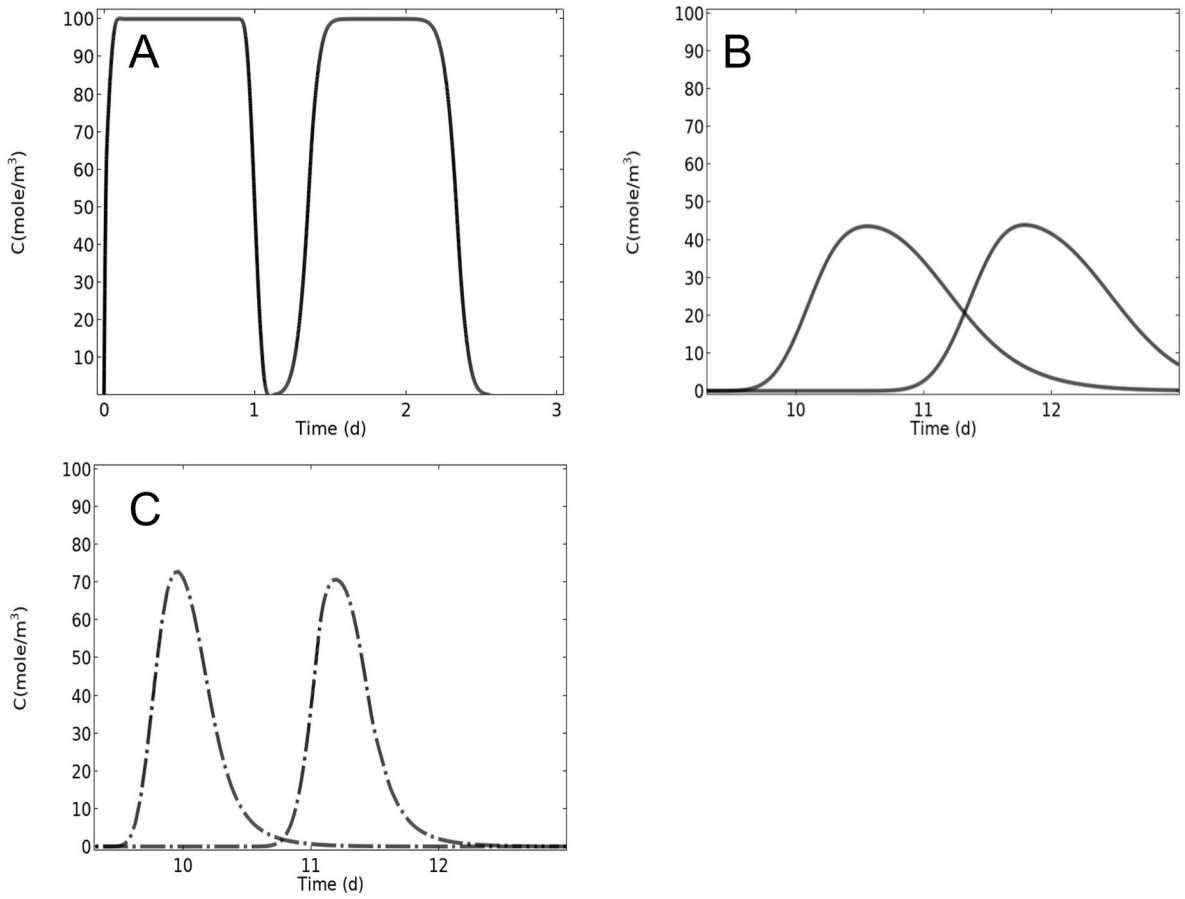

Fig. 10. Effect of dispersion in the wellbore on the tracer production curves calculated as discussed in Appendix B. The concentration change due the difference in oil saturation between wellbore (0%) and target formation (22%) is not taken into account since this doesn't alter the shape of the curves. (A) Ethyl acetate injection pulse at top and bottom of the wellbore. (B) Corresponding ethyl acetate production curves. (C) Corresponding ethanol production curves.

Kleppe (2017) with numerical software simulating a SWCT test with realistic temperature, pH changes etc. as in this paper is the best way forward towards improved S_{or} estimates.

5. Conclusions

We present the first ever model to combine realistic temperature calculations with pH dependent ethyl acetate hydrolysis rate during a SWCT test.

Our study exemplifies the useful insight that can be gained by performing numerical modeling of a SWCT test and analyzing synthetic tracer production curves. We have performed a large number of simulations to investigate how S_{or} estimates vary with different model assumptions and input data. In all simulations, both Cook (1971) formula and the mean residence time method underestimate S_{or}, typically by 2–4% - in some cases significantly more. In some cases Cook's formula yields the best result, in other cases the mean residence time is closest to the true S_{or} value.

We use a simple analytical model to calculate how the temperature of the injected brine changes smoothly with time. This yields in our opinion a more realistic temperature description than the discontinuous boundary condition applied by Park et al. (1991) and others.

Finally, we have demonstrated that dispersion in the wellbore during injection and production has a negligible impact on the tracer curves and thus S_{or} estimates with the test and formation data used in this study. This might not be the case with other input data, though.

Credit author statement

Tom Pedersen: Conceptualization, Methodology, Numerical modelling, Writing - original draft, Writing - review and editing.

Declaration of competing interest

The authors declare that they have no known competing financial interests or personal relationships that could have appeared to influence the work reported in this paper.

Acknowledgements

This work was financed by Institute for energy technology. Jan Nossen and Charlie Carlisle gave constructive criticism on an earlier version of the paper. Comments and suggestions from three anonymous reviewers are deeply appreciated.

Appendix A

We assume that the system initially is at thermal equilibrium. For this case, Ramey (1962) derived an approximate expression for the brine temperature in the wellbore, T, as a function of depth, z, and time, t:

$$T(z,t) = az + b - aA + (T_0 + aA - b)\exp\left(-\frac{z}{A}\right)$$

where z is depth, a is the geothermal gradient of the Earth, b is the surface geothermal temperature, and T_0 is the surface temperature of the injected brine. For water injection down casing,

$$A = \frac{W\mathrm{Cp,\,w}f(t)}{2\pi k}$$

in which W is the injection rate measured in kg s^{-1}, $C_{p,w}$ is the specific heat of the injected fluid and k is the thermal conductivity of the Earth. More complex expressions exist for other wellbore configurations. The function f is depicted in Ramey (1962) (his Fig. 1 – 'cylindrical source'). Fig. 3 illustrates the brine temperature as a function of time with the parameters in Table 1. It takes the tracer slug about 1.3 days to reach the target formation at 3 km depth. Then the tracer injection period commences. The temperature depicted in Fig. 3 is used as the injection temperature TI (cf. Fig. 2) in the simulations with the parameters in Table 1.

Appendix B

Taylor (1954) developed approximate solutions for the dispersion in pipes with smooth walls (as well as other configurations). For the turbulent case, he defined a virtual diffusion coefficient, δ, equal to:

$$\delta = 10.1 r_0 U\left(\frac{v^*}{U}\right)$$

where U is the average velocity of the fluid, v* is the 'friction velocity' and r_0 is the radius of the wellbore. The concentration curves can then be calculated by solving the one dimensional diffusion equation with δ.

Appendix C

https://doi.org/10.1016/j.petrol.2020.107652

References

Al-Abbad, M., Sanni, M., Kokal, S., Krivokapic, A., Dye, C., Dugstad, Ø., Hartvig, S., Huseby, O., 2016. A step-change for Single Well Chemical Tracer Tests SWCTT: field pilot testing of new sets of novel tracers. SPE-181408-MS. In: SPE Annual Technical Conference and Exhibition, Dubai, UAE, 26-28 Sept.

Al-Mutairi, F., Tiwari, S., Baroon, B., Abdullah, M., Pathak, A., Gammiero, A., 2015. Simulation of single well chemical tracer tests conducted in carbonate reservoir. SPE. https://doi.org/10.2118/175282-MS.

Al-Shalabi, E.W., Luo, H., Delshad, M., Sepehrnoori, K., 2017. Single-well chemical tracer modeling of low salinity water injection in carbonates. SPE. https://doi.org/10.2118/173994-MS.

Asakawa, K., 2005. A Generalized Analysis of Partitioning Interwell Tracer Tests. PhD dissertation. The University of Texas at Austin.

Bandura, A.V., Lvov, S.N., 2006. The ionization constant of water over wide ranges of temperature and density. J. Phys. Chem. Ref. Data 35 (1), 15–30.

Bear, J., 1979. Hydraulics of Groundwater. McGraw-Hill, p. 569.

Causin, E., Rochon, J., Marzorati, D., 1990. Field measurements of remaining oil saturation. SPE/DOE 20260, 847–855.

Chang, M.M., Maerefat, N.L., Tomutsa, L., Honarpour, M.M., 1988. Evaluation and comparison of residual oil determination techniques. SPE Form. Eval. 3 (1), 251–262.

Coats, K.H., Smith, B.D., 1964. Dead-end pore volume and dispersion in porous media. SPE J. 231, 73–84. Trans. AIME.

Comsol Multiphysics, 2018. User Guide.

Cook, C.E. Jr, 1971. Method of determining fluid saturations in reservoirs. US patent No. 3,590,923.

Deans, H.A., 1971. Method of determining fluid saturations in reservoirs. U.S. Patent 3,623,842.

Deans, H.A., Majoros, S., 1980. The Single-Well Chemical Tracer Method for Measuring Residual Oil Saturation. Final Report. U.S. Department of energy, p. 119.

Deans, H.A., Carlisle, C.T., 1986. Single-well Tracer Tests in Complex Pore Systems. SPE/DOE, p. 14886.

Deans, H.A., Ghosh, R., 1994. pH and reaction rate changes during single-well chemical tracer tests. SPE. https://doi.org/10.2118/27801-MS.

Deans, H.A., Carlisle, C., 2007. The single-well chemical tracer test – a method for measuring reservoir fluid saturations in situ. Petrol. Eng. Handbook. In: Lake, L.W. (Ed.). In: Holstein, E.W. (Ed.), Res. Eng. Petrophys, vol. 5. SPE, pp. 615–649.

Gadgil, A.G., 1979. The Single-Well Chemical Tracer Test in Petroleum Reservoirs with Multicomponent, Two-phase Flow Effects. PhD thesis. Rice University.

Ghosh, R.S., 1994. Effects of pH on Tracer Reaction (Ester Hydrolysis) Rate in Single Well Chemical Tracer Test for Residual Oil Saturation – a Quantitative Approach. Master thesis. University of Wyoming.

Huseby, O., Zarruk, G.A., Callegaro, C., Bartosek, M., 2016. Assessing oil saturation from single well chemical tracer tests by assisted history matching. SPE-179788-MS. In: SPE EOR Conf. At Oil and Gas West Asia, Muscat, Oman, 21-23 March.

Høgnesen, E.J., Strand, S., Austad, T., 2005. Waterflooding of Preferential Oil-Wet Carbonates: Oil Recovery Related to Reservoir Temperature and Brine Composition. SPE 94166.

International Critical Tables, 1930. Natl. Research Council, first ed. McGraw-Hill Book Co. Inc., New York City, VII, pp. 128–141.

Jerauld, G.R., Mohammadi, H., Webb, K.J., 2010. Interpreting single well chemical tracer tests. In: SPE Paper 129724. SPE Improved Oil Recovery Symposium, 24-28 April, Tulsa, Oklahoma, USA.

Jin, L., Jamili, A., Harwell, J.H., 2015. Modelling and interpretation of Single Well Tracer Tests (SWCTT) for pre and post chemical EOR in two high salinity reservoirs. In: SPE Paper 173618-MS.

Khalediallidusti, R., Kleppe, J., 2015. Numerical interpretation of single well chemical tracer (SWCT) tests to determine residual oil saturation in Snorre Reservoir. SPE-174378-MS. In: EUROPEC 2015, Madrid, Spain, 1-4 June.

Khalediallidusti, R., Kleppe, J., 2017. A comprehensive framework for the theoretical assessment of the single-well-chemical-tracer tests. J. Petrol. Sci. Eng. 159, 164–181.

Khalediallidusti, R., Kleppe, J., 2018. Significance of geochemistry in single-well chemical-tracer tests by coupling a multiphase-flow simulator to the geochemical package. SPE J. 1126–1144.

Khalediallidusti, R., Kleppe, J., Enayatpour, S., 2014. Evaluation and comparison of available tracer methods for determining residual oil saturation and developing an innovative single well tracer technique: dual salinity tracer. In: International Petroleum Technology Conference. https://doi.org/10.2523/IPTC-17990-MS.

Millington, R.J., Quirk, J.M., 1961. Permeability of porous solids. Trans. Faraday Soc. 57, 1200–1207.

Park, Y.J., 1989. Thermal Effects of Single-Well Chemical Tracer Tests for Measuring Residual Oil Saturation. PhD Thesis. University of Houston, p. 209.

Park, Y.J., Deans, H.A., Tezduyar, T.E., 1990. Finite element formulation for transport equations in a mixed co-ordinate system: an application to determine temperature effects on the single-well chemical tracer test. Int. Jour. Num. Methods in fluids 11, 769–790.

Park, Y.J., Deans, H.A., Tezduyar, T.E., 1991. Thermal effects on single-well chemical tracer tests for measuring residual oil saturation. SPE Form. Eval. 6, 401–408.

Pedersen, T., 2018. Properly designed temperature history nanoparticles may improve residual oil saturation estimates from SWCT tests. J. Petrol. Sci. Eng. 170, 383–391.

Ramey Jr., H.J., 1962. Wellbore heat transmission. SPE J. Petrol. Techn. 96, 427–435.

Salathiel, R.A., 1973. Oil recovery by surface film drainage in mixed-wettability rocks. Trans. AIME 225, 1216–1224.

Sheely, C.Q., Baldwin, D.E., 1982. Single-well tracer tests for evaluating chemical enhanced oil recovery processes. J. Petrol. Technol. 1887–1896.

Shook, G.M., Pope, G.A., Asakawa, K., 2009. Determining reservoir properties and flood performance from tracer test analysis. SPE 124614.

Taylor, G., 1954. The dispersion of matter in turbulent flow through a pipe. Proc. Roy. Soc. Lond. A 223, 446–468.

Teklu, T.W., Brown, J.S., Kazemi, H., Graves, R.M., AlSumati, A.M., 2013. A critical literature review of laboratory and field scale determination of residual oil

saturation. In: SPE 164483. SPE Prod. Operat. Symp., Oklahoma City, Oklahoma, 23-26 March.
Tezduyar, T.E., Park, Y.J., Deans, H.A., 1987. Finite element procedures for time-dependent convection-diffusion-reaction systems. Int. J. Numer. Methods Fluid. 7, 1013–1033.
Tomich, J.F., Dalton Jr., R.L., Deans, H.A., Shallenberger, L.K., 1973. Single-well tracer method to measure residual oil saturation. J. Petrol. Geol. 211–218.
Wellington, S.L., Richardson, E.A., 1994a. Redesigned ester single-well tracer test that incorporates pH-driven hydrolysis rate changes. SPE Res. Eng. 233–239.
Wellington, S.L., Richardson, E.A., 1994b. Simultaneous Use of ester and CO_2 Single-Well Tracers. SPE Res. Eng, pp. 240–246.